

Accurate Determination of the Band-Gap Energy of the Rare-Earth Niobate Series

Alka B. Garg^{1,2}, David Vie³, Placida Rodriguez-Hernandez⁴, Alfonso Muñoz⁴, Alfredo Segura⁵, Daniel Errandonea^{5,*}

¹High Pressure and Synchrotron Radiation Physics Division, Bhabha Atomic Research Centre, Mumbai 400085, India

²Homi Bhabha National Institute, Anushaktinagar, Mumbai 400094, India

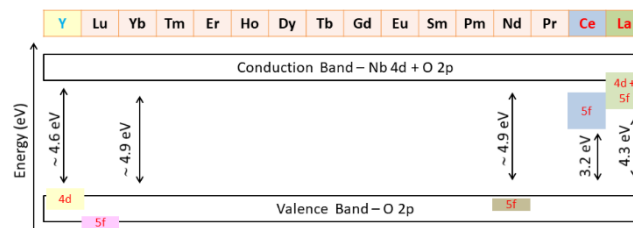
³Institut de Ciència dels Materials de la Universitat de València, Apartado de Correos 2085, E-46071 València, Spain

⁴Departamento de Física, Instituto de Materiales y Nanotecnología, MALTA Consolider Team, Universidad de La Laguna, La Laguna, E-38204 Tenerife, Spain

⁵Departamento de Física Aplicada-ICMUV, MALTA Consolider Team, Universidad de Valencia, Edificio de Investigación, Carrer del Dr. Moliner 50, Burjassot, 46100 Valencia, Spain

Abstract: In this work, we report diffuse reflectivity measurements in InNbO_4 , ScNbO_4 , YNbO_4 , and eight different rare-earth niobates. From a comparison with the established values of the band gap of InNbO_4 and ScNbO_4 , we have found that the broadly used Tauc plot analysis leads to erroneous estimates of the band-gap energy of niobates. In contrast, accurate results are obtained considering excitonic contributions using the Elliot-Toyozawa model. We have found that YNbO_4 and the rare-earth niobates are wide band-gap materials. The band-gap energy is 3.25 eV for CeNbO_4 , 4.35 eV for LaNbO_4 , 4.5 eV for YNbO_4 , and 4.73 – 4.93 eV for SmNbO_4 , EuNbO_4 , GdNbO_4 , DyNbO_4 , HoNbO_4 , and YbNbO_4 . An explanation for the obtained results will be presented. The fact that the band-gap energy is nearly not affected by the rare-earth substitution from SmNbO_4 to YbNbO_4 and the circumstance that these are the compounds with the largest band gap are a consequence of the fact that the band structure near the Fermi level originates mainly from Nb 4d and O 2p orbitals. We hypothesize that YNbO_4 , CeVO_4 , and LaNbO_4 have smaller band gaps because of the contribution from rare-earth atom 4d or 5f states to the states near the Fermi level.

TOC IMAGE



KEYWORDS: Rare-earth niobate, band gap, reflectance, electronic properties

Rare-earth and trivalent metals niobates (MNbO_4) have been used for half a century as luminescent materials [1]. These compounds crystallize in the monoclinic fergusonite structure (space group $I2_1/a$ also described with other settings as $I2_1/b$ or $C2/c$) and have exceptional chemical stability, luminescent, and dielectric properties, and ion conductivities [2]. Because of it, they have been proposed for many different multifunctional applications. They include lasers, light emitters, capacitors, optical fibers, medical applications, temperature detectors, bioimaging, photocatalysts for both contaminant degeneration and H_2 generation, chemically robust hosts for nuclear materials and wastes, ion conductors for lithium batteries, or solid-oxide fuel cells, among others [2 – 6]. The fact that MNbO_4 niobates can be obtained as single crystals [7] and nanocrystals [8] give them a great versatility regarding applications. One of the applications of MNbO_4 niobates that has been gaining momentum in the last years is their use for environmentally friendly white-light-emitting diodes (LEDs) [9, 10]. In the last years, these devices have replaced in the market the conventional light sources, including Edison's incandescent lamp and the Hg-discharge-based fluorescent lamp. LEDs have many advantages over the other light sources, including lower power consumption, longer lifetime, improved physical robustness, smaller size, and faster switching [11]. One of the crucial facts to further optimize white LEDs based on orthoniobates, it is the precise determination of the energy of their electronic band gap (E_g), which is lacking yet. Several efforts have been devoted to it, but the information in the literature [2, 4, 5, 12 – 16] is scarce and in some cases, contradictory as can be seen in Table 1. Notice that band-gap values from 2.9 to 5.04 eV have been reported for orthoniobates. Such a large variation of E_{gap} is in contradiction with the know-systematic of related orthovanadates, which have been extensively studied [17, 18]. In special, in YNbO_4 ($E_{\text{gap}} = 3.7 - 4.96$ eV), LuNbO_4 ($E_{\text{gap}} = 4.2 - 5.04$ eV), and GdNbO_4 ($E_{\text{gap}} = 3.48 - 4.89$ eV) there are significant discrepancies in the literature. These facts indicate that a systematic study of the band-gap energy of MNbO_4 niobates is timely. Here we report diffuse reflectance measurements in YNbO_4 , LaNbO_4 , CeNbO_4 , SmNbO_4 , EuNbO_4 , GdNbO_4 , DyNbO_4 , HoNbO_4 , and YbNbO_4 . A systematic analysis of the results using an Elliot-Toyozawa model [19, 20] has allowed us to accurately determine the band-gap energy of the studied compounds. It allows us also to conclude that the traditional method of determination based on the Tauc plot [21] underestimates the band-gap

energy. Our method for the determination of E_g has been validated by performing diffuse reflectance measurements in InNbO_4 and ScNbO_4 , giving an excellent agreement with the established band-gap values, 4.7 and 4.8 eV, respectively [22, 23]. From our study, we conclude that the most studied compounds have a band-gap energy of 4.73 – 4.93 eV, having only CeNbO_4 (3.25 eV), LaNbO_4 (4.35 eV), and YNbO_4 (4.55 eV) narrower band gaps. The observed results will be explained using available band-structure calculations.

Let us start presenting results from InNbO_4 and ScNbO_4 , which have been used to establish the method used to determine E_g . Both materials have a monoclinic wolframite-type structure (related to fergusonite) and their band-gap energies have been accurately determined previously [22, 23]. In Fig. 1 we present the absorption spectra $F(R_\infty)$ obtained from the diffuse-reflectance measurement via the Kubelka–Munk transformation [24], which can be considered approximately proportional to the absorption coefficient (α) [25]. In both InNbO_4 and ScNbO_4 , the absorbance has a sharp absorption onset above 4 eV, reaching a maximum at 4.7 and 4.75 eV, respectively (see Fig. 1). In the literature, there is an agreement that InNbO_4 and ScNbO_4 have direct band gaps with $E_{\text{gap}} = 4.7$ and 4.8 eV, respectively. However, if we analyze our results using the traditional Tauc plot analysis [21], determining E_g from a linear least-squares fit to zero in $(hvF(R_\infty))^2$ versus hv (as shown in Fig. 1), we found values for E_{gap} which underestimate by 0.4 eV from the established values of E_{gap} . We are not surprised by this fact because this method has been recently challenged [26]. The main drawback is that it tends to underestimate the band-gap energy in materials showing sub-band-gap absorption tails related to defects, surface effects, and other phenomena which are reflected in the absorption spectrum as an Urbach tail [26]. The fact that the Tauc analysis neglects the presence of excitons could also lead to the underestimation of E_{gap} [27]. In materials related to MNbO_4 niobates, like InVO_4 , the application of the traditional Tauc plot analysis leads to underestimations of up to 1.8 eV in the value of E_g [28]. Then, it is not surprising that in InNbO_4 and ScNbO_4 , it could lead to an underestimation of 0.4 eV. We will show now that this is because of the excitonic contribution to the fundamental absorption spectrum. In InNbO_4 and ScNbO_4 the steplike absorption present above 4 eV (see Fig. 1) is typical of direct transitions in which

excitonic effects are observed even at room temperature [29]. This can be confirmed by fitting the absorbance obtained by means of the excitonic Elliott-Toyozawa model [19, 20] where:

$$F(R_\infty) \propto \alpha(h\nu)$$

$$\propto \frac{1}{h\nu} \left[\sum_j \frac{2E_B}{j^3} \operatorname{sech}\left(\frac{h\nu - E_j^B}{\Gamma}\right) + \int_{E_g}^{\infty} \operatorname{sech}\left(\frac{h\nu - E}{\Gamma}\right) \frac{1}{1 - \exp(-2\pi \sqrt{\frac{E_g}{E - E_g}})} dE \right]$$

In this expression, the first term within the brackets is the discrete excitonic contribution, and the second term is the continuum contribution. In our fitting we have assumed that only the fundamental exciton state ($j = 1$) contributes to the peak, being $E_1^B = E_{gap} - E_B$, where E_B is the exciton binding energy. The only fitting parameters are E_g , E_B , and Γ , which takes the spectral linewidth into account. This simple model can reproduce the absorbance of the two compounds as it can be seen in Fig. 1. From our fit we have determined $E_{gap} = 4.7$ for InNbO_4 and 4.8 eV for ScNbO_4 . These values are in excellent agreement with the literature [22, 23]. The obtained values for E_B are 70 and 120 meV, respectively. These values are comparable to the exciton binding energy of wide band-gap oxides [29]. The excellent agreement with the literature and the good quality of fits (using a simple model with only the fundamental exciton) confirm that excitonic contributions are important in the absorbance of MNbO_4 niobates. We consequently will use the same model to analyze all the rare-earth niobates we have investigated.

Once the correct method for determining the band-gap energy has been established we will present the results on rare-earth niobates. We will first present SmNbO_4 , EuNbO_4 , and GdNbO_4 . The results of our experiments and the analysis are provided in Fig. 2. The three compounds have a sharp absorption edge typical of a direct band gap. Below that energy, there is a sub-band-gap Urbach tail, typical of MXO_4 [30] oxides and weak peaks which can be attributed to internal 4f-4f transitions associated to the lanthanide cation [31, 32]. By applying the Elliott-Toyozawa model the

fundamental absorption edge can be fitted quite well. The determined band-gap energies are 4.95, 4.73, and 4.93 eV for SmNbO₄, EuNbO₄, and GdNbO₄, respectively. The obtained values for the exciton binding energy (see Fig. 2) are comparable to the values determined for InNbO₄ and ScNbO₄. The band-gap energy is very close to the energy of the maximum of $F(R_\infty)$ as shown in Fig. 2. In the figure, we also include a fit using the Tauc plot. The values estimated for E_{gap} with this method is always more than 0.4 eV compared to the correct value as can be seen in Table 1. In this table, we also compare our results with previous studies. For SmNbO₄, this is the first determination of E_{gap} , the value obtained is consistent with photoluminescence measurements, that constrain the band-gap energy to 4.7-5.0 eV [33]. In the case of GdNbO₄, our result (4.93 eV) is in excellent agreement with the results of Feng et al. (4.89 eV) [12]. This indicates that the band gap of 3.48 eV reported by Hirano et al. is an underestimation. The same can be stated by the band gap of 3.45 eV determined by the same authors for EuNbO₄ [12], which is 1.3 eV smaller than the value of E_{gap} determined in the present work.

In Fig. 3 we present the results obtained from DyNbO₄, HoNbO₄, and YbNbO₄. Again, the three compounds have a very large band gap $E_{\text{gap}} \sim 4.9$ eV (see Fig. 3 and Table 1). In Fig. 3 it can also be seen that the band-gap energy is very close to the energy of the maximum of $F(R_\infty)$. The figure also shows how E_{gap} is underestimated by ~ 0.4 eV when the Tauc plot analysis is applied. Notice that E_{gap} in the three compounds is very similar to E_{gap} in SmNbO₄, EuNbO₄, and GdNbO₄. As we will explain towards the end of the manuscript, this is a consequence of the fact that the electronic states at the bottom of the conduction band and the top of the valence band are dominated by O 2p states and Nb 4d states. Thus, as a first approximation, the band gap is determined by the configuration of the NbO₄ tetrahedron, which does not change significantly from one compound to the other. The three of them also have the typical Urbach tail plus a contribution from absorptions from the 4f levels of the rare-earth atoms. In addition, HoNbO₄ and DyNbO₄ have in $F(R_\infty)$ sub-band-gap sharp absorptions caused by internal 4f-4f transitions of Dy and Ho [32]. For DyNbO₄ and HoNbO₄, this is the first time that the band-energy is reported. In YbNbO₄, our result ($E_{\text{gap}} = 4.9$ eV) shows that E_{gap} has been largely underestimated in a previous report [16].

In Fig. 4, we present the results obtained from YNbO₄, LaNbO₄, and CeNbO₄. The figure shows that the Tauc analysis always gives underestimated values of E_{gap} .

According to the Elliot-Toyozawa model, YNbO_4 has a band-gap energy of 4.56 eV (see Fig. 4 and Table 1). This value is 10% smaller than in the previously discussed niobates, and it is comparable to the maximum value of E_{gap} reported in previous studies [2, 4, 5, 14]. For LaNbO_4 , we have determined E_{gap} 4.35 eV. The previously determined value was 10% smaller [13]. For CeNbO_4 , this is the first time that E_{gap} is determined. The obtained value, 3.25 eV, indicates that this compound is the orthoniobate with the smallest band gap. As in the other studied compounds, in the three compounds presented in Fig. 4, the band-gap energy is very close to the energy of the maximum of $F(R_\infty)$.

It is interesting to stress that the band-gap energy of rare-earth niobates follows a very similar trend as observed for rare-earth vanadates [17, 34, 35]. In the vanadates, except for LaVO_4 and CeVO_4 , all the members of the family have a band gap close to 3.8 eV. LaVO_4 has a band gap of 3.5 eV and CeVO_4 a band gap of 3.2 eV. The 3.8 eV band gap is a consequence of the fact that states near the Fermi level are dominated by O 2p and V 3d states. In the other compounds, the band gap is reduced due to the contribution of 5d and 4f electrons from La and Ce. A similar picture provides a qualitative explanation to the results reported here. The band structure and electronic density of states (DOS) of most niobates are reported in the literature [2, 13, 36, 37, 38]. They are qualitatively similar to the band structure and DOS of vanadates [34], having the band structures a similar topology and the states near the Fermi level a similar composition. According to band-structure calculations, the studied niobates have an indirect gap, but the difference with the direct band gap is smaller than 0.1 eV [2, 13, 36, 37, 38]. Then the absorption edge will be dominated by the direct band-gap and $F(R_\infty)$ can be analyzed assuming a direct band gap as it has been done in this work.

To provide a more quantitative discussion, we will focus on LaNbO_4 , CeNbO_4 , EuNbO_4 , and YbNbO_4 [38], which are representative of the family of fergusonite-type niobates. In the four compounds, the minimum of the conduction band (CB) and the maximum of valence band (VB) are located at V and Γ point of the Brillouin zone. However, there is a Γ - Γ direct band gap very close in energy. According to the electronic DOS, in EuNbO_4 and YbNbO_4 the valence-band maximum is dominated by O 2p states. This behavior is typical of most wide-band-gap oxides. On the other hand, the conduction-band minimum is predominantly dominated by Nb 4d states with a small contribution of O 2p states. This molecular orbital composition is analogous to what

happens in vanadates with V 3d and O 2p states [34] and in other ternary oxides like tungstates (molybdates) with W (Mo) 5d (4d) and O 2p states [39]. Consequently, the configuration of the NbO₄ tetrahedron, the coordination polyhedron of Nb in fergusonite, will have a determinant role in determining the band-gap energy. Interestingly, this unit is little modified when going from one compound to the other, changing the average Nb-O bond distance less than 1% along the series of rare-earth niobates. Then, it is not surprising that most members of this family have a very similar E_{gap}. It is also not surprising that these compounds have a band-gap energy comparable to that of Nb₂O₅ (E_{gap} = 5.1 eV) in which states at the bottom of the CB and top the VB are also dominated by the hybridization of O 2p and Nb 4d states, and O 2p states, respectively [40]. The reason to the band-gap energy closing of LaNbO₄ and CeNbO₄ comes from the fact that these are the only two compounds where the lanthanide orbitals contribute to the conduction band. Exactly as happens in LaVO₄ and CeVO₄, the vanadates with the smallest band-gap energy [17].

Summing up, in this letter we reported diffuse reflectance measurements for rare-earth niobates and proposed a method for accurately determining their band-gap energy. We have shown that in most previous studies the band-gap energy has been underestimated. The band-gap energy of the studied compounds is 3.25 eV for CeNbO₄, 4.35 eV for LaNbO₄, 4.5 eV for YNbO₄, and 4.73 – 4.93 eV for SmNbO₄, EuNbO₄, GdNbO₄, DyNbO₄, HoNbO₄, and YbNbO₄. We also provide an explanation to the experimental results based on density functional calculations. The reported information is crucial for technological applications of rare-earth niobates.

METHODS

Experimental details: Polycrystalline rare-earth niobates were synthesized by the commonly used solid-state reaction technique. Starting metal oxides, R₂O₃ and Nb₂O₅ (purity > 99.9%) were pre-dried to remove any moisture or organic impurities. These dried binary oxides were weighed in stoichiometric (1:1) ratio, followed by hand mixing in pestle and mortar, cold pressing into cylinders of 12.5 mm in diameter and 5 mm in height, and fired at 1200 °C for 24 hrs. in a box type programmable resistive furnace. These pellets were further sintered at 1300 °C for 48 hrs. Single phase formation of the

compound was confirmed by angle-dispersive powder x-ray diffraction. We confirmed that all synthesized rare-earth niobates crystallize in the fergusonite structure. For measurements in ScNbO_4 and InNbO_4 , we used the same samples used in previous studies [21, 22]. For the diffuse reflectance measurements, powder samples were manually grounded in an agata mortar, placed in the sample holder, and supported with a quartz window. Measurements were carried out on a Shimadzu UV-Vis 2501PC spectrophotometer equipped with an integrating sphere for diffuse reflectance measurements. BaSO_4 was used as reference material and for background measurement. The spectral range covered by measurements was 220-900 nm, with a resolution of 1 nm and a Spectral bandwidth of 5 nm. The spectra recorded in %R were transformed using the Kubelka-Munk function [24].

AUTHORS INFORMATION

Corresponding Author

*E-mail: daniel.errandonea@uv.es

ORCID: 0000-0003-0189-4221

Author Contributions

A.B.G. synthesizes the samples. D.V. performed the diffuse reflectance measurements. D.E. designed the study and carried out the data analysis. All authors contribute to the discussion, writing, and proofreading and have given approval to the final version of the manuscript.

Funding Sources

Spanish Mineco (MINECO/AEI/0.13039/501100003329) Project No. RED2018-102612-T, Spanish MCIN (MCIN/AEI/10.13039/501100011033) Projects No. PID2019-106383GB-41/43, Generalitat Valencina Project No. PROMETEO CIPROM/2021/075 (GREENMAT), and Advanced Materials Programme supported by MCIN with funding from European Union NextGenerationEU (PRTR-C17.I1) Project MFA/2022/007.

Notes

The authors declare no competing financial interest.

ACKNOWLEDGMENTS

This study was supported by the MALTA Consolider Team network (Project No. RED2018-102612-T), financed by MINECO/AEI/0.13039/501100003329, the I+D+i Project No. PID2019-106383GB-41/43 financed by MCIN/AEI/10.13039/501100011033, as well as by the Project No. PROMETEO CIPROM/2021/075 (GREENMAT) financed by Generalitat Valenciana. This study forms part of the Advanced Materials Programme and was supported by MCIN with funding from European Union NextGenerationEU (PRTR-C17.11) and by Generalitat Valenciana under grant MFA/2022/007. The authors also thank Prof. Ana Costero from Dept. de Química Orgánica at Univ. de Valencia for letting us use the Shimadzu UV-Vis 2501PC spectrophotometer for diffuse reflectance measurements.

REFERENCES

- [1] Blasse, G.; Bril, A. Luminescence phenomena in compounds with fergusonite structure, *J. Lumin.* **1970**, *3*, 109–131.
- [2] Ding, D.; Zhang, H.; Liu, W.; Sun, D.; Zhang, Q. Experimental and first principle investigation the electronic and optical properties of YNbO₄ and LuNbO₄ phosphors, *J. Mater. Science: Materials in Electronics* **2018**, *29*, 11878–11885.
- [3] Graça, M.P.F.; Peixoto, M.V.; Ferreira, N.; Rodrigues, J.; Nico, C.; Costa F.M.; Monteiro, T. Optical and dielectric behaviour of EuNbO₄ crystals, *J. Mater. Chem. C* **2013**, *1*, 2913-2919.
- [4] Feng, Z.; Lou, B.B.; Chen, Q.; Yin, M.; Ma, C.G.; Duan, C.K. Self-Activated and Bismuth-Related Photoluminescence in Rare-Earth Vanadate, Niobate, and Tantalate Series: A First-Principles Study, *Inorg. Chem.* **2021**, *60*, 16614–16625.
- [5] Hirano, M; Dozono, H. Hydrothermal formation and characteristics of rare-earth niobate phosphors and solid solutions between YNbO₄ and TbNbO₄, *Mat. Chem. Phys.* **2014**, *143*, 860-866.
- [6] Nyman, M.; Rodriguez, M.A.; Rohwer, L.E.S.; Martin, J.E.; Waller, M.; Osterloh, F.E. Unique LaTaO₄ Polymorph for Multiple Energy Applications, *Chem. Mater.* **2009**, *21*, 4731–4737.
- [7] Fulle, K.; McMillen, C.D.; Sanjeewa, L.D.; Kolis, J.W. Hydrothermal Chemistry and Growth of Fergusonite-type RENbO₄ (RE = La–Lu, Y) Single Crystals and New Niobate Hydroxides, *Cryst. Growth Des.* **2016**, *16*, 4910–4917.

- [8] Hirano, M.; Dozono, H. Direct Formation and Luminescence Properties of Yttrium Niobate YNbO₄ Nanocrystals via Hydrothermal Method, *J. Amer. Cer. Soc.* **2013**, *96*, 3389-3393.
- [9] Liu, X.; Lü, Y.; Chen, C.; Luo, S.; Zeng, Y.; Zhang, X.; Shang, M.; Li, C.; Lin, J. Synthesis and Luminescence Properties of YNbO₄:A (A = Eu³⁺ and/or Tb³⁺) Nanocrystalline Phosphors via a Sol–Gel Process, *J. Phys. Chem. C* **2014**, *118*, 27516–27524.
- [10] Lü, Y.; Tang, X.; Yan, L.; Li, K.; Liu, X.; Shang, M.; Li, C.; Lin, J. Synthesis and Luminescent Properties of GdNbO₄:RE³⁺ (RE = Tm, Dy) Nanocrystalline Phosphors via the Sol–Gel Process, *J. Phys. Chem. C* **2013**, *117*, 21972-21980.
- [11] Lin, C.C.; Liu, R.S. Advances in Phosphors for Light-emitting Diodes, *J. Phys. Chem. Lett.* **2011**, *2*, 1268–1277,
- [12] Hirano, M.; Ishikawa, K. Direct synthesis of nanocrystalline GdNbO₄ and GdNbO₄-based phosphors doped with Eu³⁺ through hydrothermal route, *J. Cer. Soc. Japan* **2016**, *124*, 42-48.
- [13] Arai, M.; Xu, Y.; Kohiki, S.; Matsuo, M.; Shimooka, H.; Shishido, T.; Oku, M. Dielectric Property and Electronic Structure of LaNbO₄, *Jap. J. Appl. Phys.* **2005**, *44*, 6596-6599.
- [14] Lee, S.K.; Chang, H.; Han, C.H.; Kim, H.J.; Jang, H.G. Park, H.D. Electronic Structures and Luminescence Properties of YNbO₄ and YNbO₄:Bi, *J. Solid State Chem.* **2001**, *156*, 267-273.
- [15] Peixoto, J.C.; Dias, A., Matinaga, F.M.; Siqueira, K.P.F. Luminescence properties of PrNbO₄ and EuNbO₄ orthoniobates and investigation of their structural phase transition by high-temperature Raman spectroscopy, *J. Lumin.* **2021**, *238*, 118284.
- [16] Zhang, Z.; Guo, L.; Sun, H.; Peng, D.; Zou, H.; Sun N.; Zhang, Q.; Hao, X. Rare earth orthoniobate photochromics with self-activated upconversion emissions for high-performance optical storage applications, *J. Mater. Chem. C* **2021**, *9*, 13841-13850
- [17] Errandonea, D. High pressure crystal structures of orthovanadates and their properties, *J. Appl. Phys.* **2020**, *128*, 040903.
- [18] Errandonea, D.; Garg, A.B. Recent progress on the characterization of the high-pressure behaviour of AVO₄ orthovanadates, *Prog. Mat. Science* **2018**, *97*, 123-169.
- [19] Elliott, R.J. Intensity of optical absorption by excitons, *Phys. Rev.* **1957**, *108*, 1384–1389.
- [20] Toyozawa, Y. Theory of Line-Shapes of the Exciton Absorption Bands, *Prog. Theor. Phys.* **1958**, *20*, 53-81.
- [21] Tauc, J. Optical properties and electronic structure of amorphous Ge and Si, *Mat. Res. Bul.* **1968**, *3*, 37–46.
- [22] Botella, P.; Enrichi, F.; Vomiero, A., Muñoz-Santiuste, J.E.; Garg, A.B.; Arvind, A.; Manjón, F.J.; Segura, A.; Errandonea, D, Investigation on the Luminescence Properties

of InMO_4 ($M = \text{V}^{5+}, \text{Nb}^{5+}, \text{Ta}^{5+}$) Crystals Doped with Tb^{3+} or Yb^{3+} Rare Earth Ions, *ACS Omega* **2020**, *5*, 2148–2158.

[23] Ouahrani, T.; Garg, A.B.; Rao, R.; Rodríguez-Hernández, P.; Muñoz, A.; Badawi, M.; Errandonea, D. On the high-pressure properties of wolframite-type ScNbO_4 , *J. Phys. Chem. C* **2022**, *126*, 4664–4676.

[24] Kubelka, P.; Munk, F. An article on optics of paint layers, *Z. Tech. Phys.* **1931**, *12*, 593–603.

[25] Dolgonos, A., Mason; T.O.; Poeppelmeier, K.R. Direct optical band gap measurement in polycrystalline semiconductors: A critical look at the Tauc method, *J. Solid State Chem.* **2016**, *240*, 43–48.

[26] Makuła, P.; Pacia, M.; Macyk; W. How to correctly determine the band gap energy of modified semiconductor photocatalysts based on UV–Vis spectra, *J. Phys. Chem. Lett.* **2018**, *9*, 6814–6817.

[27] Ruf, F.; Aygüler, M.F.; Giesbrecht, N.; Rendenbach, B.; Magin, A.; Docampo, P.; Kalt, H.; Hetterich, M. Temperature-dependent studies of exciton binding energy and phase-transition suppression in $(\text{Cs,FA,MA})\text{Pb}(\text{I,Br})_3$ perovskites, *APL Mater.* **2019**, *7*, 031113

[28] Botella, P.; Errandonea, D.; Garg, A.B.; Rodríguez-Hernández, P.; Muñoz, A.; Achary, S.N.; Vomiero, A. High-pressure characterization of the optical and electronic properties of InVO_4 , InNbO_4 , and InTaO_4 , *SN Applied Sciences* **2019**, *1*, 389.

[29] Segura, A.; Artús, L.; Cuscó, R.; Goldhahn, R.; Feneberg, M. Band gap of corundumlike $\alpha\text{-Ga}_2\text{O}_3$ determined by absorption and ellipsometry, *Phys. Rev. Mat.* **2017**, *1*, 024604.

[30] Errandonea, D.; Muñoz, A.; Rodríguez-Hernández, P.; Proctor, J.E.; Sapiña, F.; Bettinelli, M. Theoretical and Experimental Study of the Crystal Structures, Lattice Vibrations, and Band Structures of Monazite-Type PbCrO_4 , PbSeO_4 , SrCrO_4 , and SrSeO_4 , *Inorg. Chem.* **2015**, *54*, 7524–7535.

[31] Carnall, W. T.; Crosswhite, H.; Crosswhite, H. M. Energy Level Structure and Transition Probabilities in the Spectra of the Trivalent Lanthanides in LaF_3 ; Argonne, IL (United States), 1978.

[32] Bandiello, E.; Errandonea, D.; Piccinelli, F.; Bettinelli, M.; Díaz-Anichtchenko, D.; Popescu, C.; Characterization of Flux-Grown $\text{Sm}_x\text{Nd}_{1-x}\text{VO}_4$ Compounds and High-Pressure Behavior for $x = 0.5$, *J. Phys. Chem. C* **2019**, *123*, 30732–30745.

[33] Nico, C.; Soares, M.R.N.; Costa, F.M.; Monteiro, T.; Graça, M.P.F. Structural, optical, and electrical properties of SmNbO_4 , *J. Appl. Phys.* **2016**, *120*, 051708.

[34] Panchal, V.; Errandonea, D.; Segura, A.; Rodríguez-Hernández, P.; Muñoz, A.; Lopez-Moreno, S.; Bettinelli, M. The Electronic Structure of Zircon-Type Orthovanadates: Effects of High-Pressure and Cation Substitution, *J. Appl. Phys.* **2011**, *110*, 043723.

- [35] Muñoz-Santiuste, J. E.; Lavín, V.; Rodríguez-Mendoza, U. R.; Ferrer-Roca, Ch.; Errandonea, D.; Martínez-García, D.; Rodríguez-Hernández, P.; Muñoz, A.; Bettinelli, M. Experimental and theoretical study on the optical properties of LaVO_4 crystals under pressure, *Phys. Chem. Chem. Phys.* **2018**, *20*, 27314-27328.
- [36] Ding, S.; Zhang, H.; Zhang, Q.; Chen, Y.; Dou, R.; Peng, F.; Liu, W.; Sun, D. Experimental and first principle study of the structure, electronic, optical and luminescence properties of M-type GdNbO_4 phosphor, *J. Sol. State Chem.* **2018**, *262*, 87-93.
- [37] Litimein, F.; Khenata, R.; Gupta, S. K.; Murtaza, G.; Reshak, A. H.; Bouhemadou, A.; Omran, S. B.; Yousaf, M.; Jha, P. K. Structural, electronic, and optical properties of orthorhombic and triclinic BiNbO_4 determined via DFT calculations, *J. Mater. Sci.* **2014**, *49*, 7809–7818.
- [38] Materials Project web site, <https://materialsproject.org/>
- [39] Liang, A.; Turnbull, R.; Rodríguez-Hernandez, P.; Muñoz, A.; Jasmin, M.; Shi, L. T.; Errandonea, D. General relationship between the band-gap energy and iodine-oxygen bond distance in metal iodates, *Phys. Rev. Materials* **2022**, *6*, 044603.
- [40] Sathasivam, S.; Williamson, B. A. D.; Althabaiti, S. A.; Obaid, A. Y.; Basahel, S. N.; Mokhtar, M.; Scanlon, D. O.; Carmalt, C. J.; Parkin, I. P. Chemical Vapor Deposition Synthesis and Optical Properties of Nb_2O_5 Thin Films with Hybrid Functional Theoretical Insight into the Band Structure and Band Gaps, *ACS Appl. Mater. Interfaces* **2017**, *9*, 18031–18038.

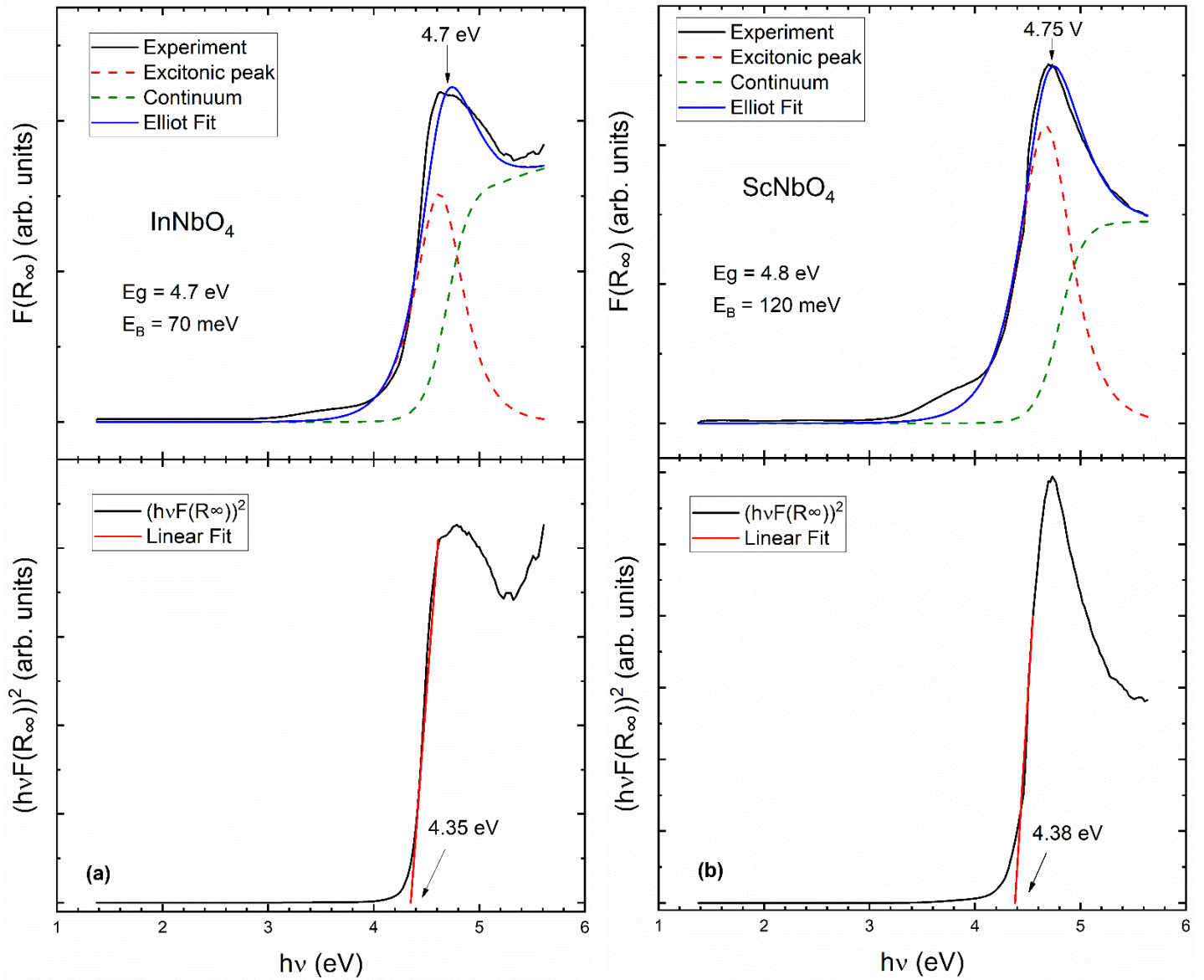


Figure 1: (a) In the top we plot the $F(R_\infty)$ spectrum of InNbO₄ together with the fit used to determine the band-gap energy. The black line is the experiment, the blue line is the fit, the green dashed line is the continuum contribution, and the red dashed line is the excitonic contribution. In the bottom we show the Tauc plot traditionally used to determine E_{gap} . (b) Same but for ScNbO₄.

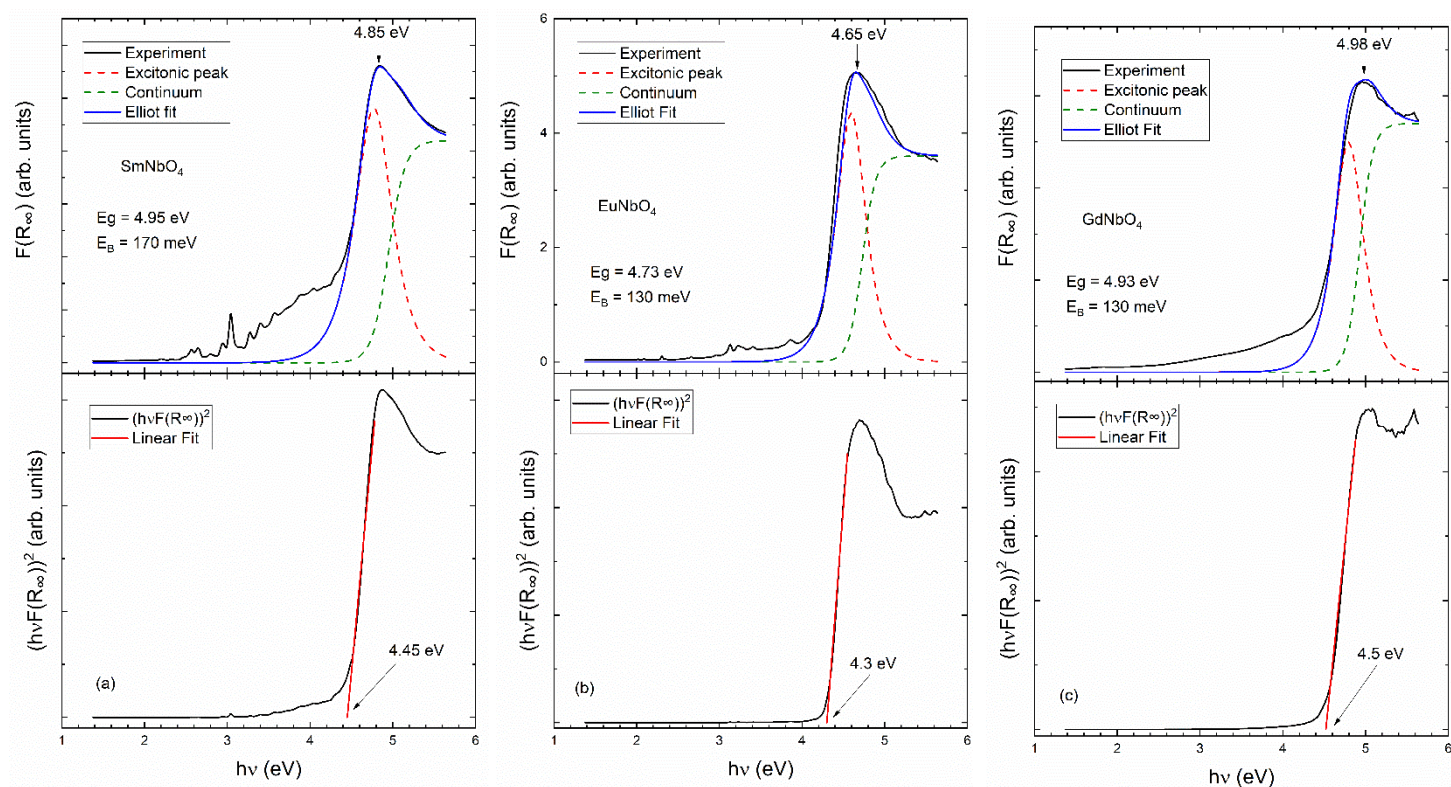


Figure 2: (a) In the top we plot the $F(R_\infty)$ spectrum of SmNbO_4 together with the fit used to determine the band-gap energy. The black line is the experiment, the blue line is the fit, the green dashed line is the continuum contribution, and the red dashed line is the excitonic contribution. In the bottom we show the Tauc plot traditionally used to determine E_{gap} . (b) Same but for EuNbO_4 . (c) Same but for GdNbO_4 .

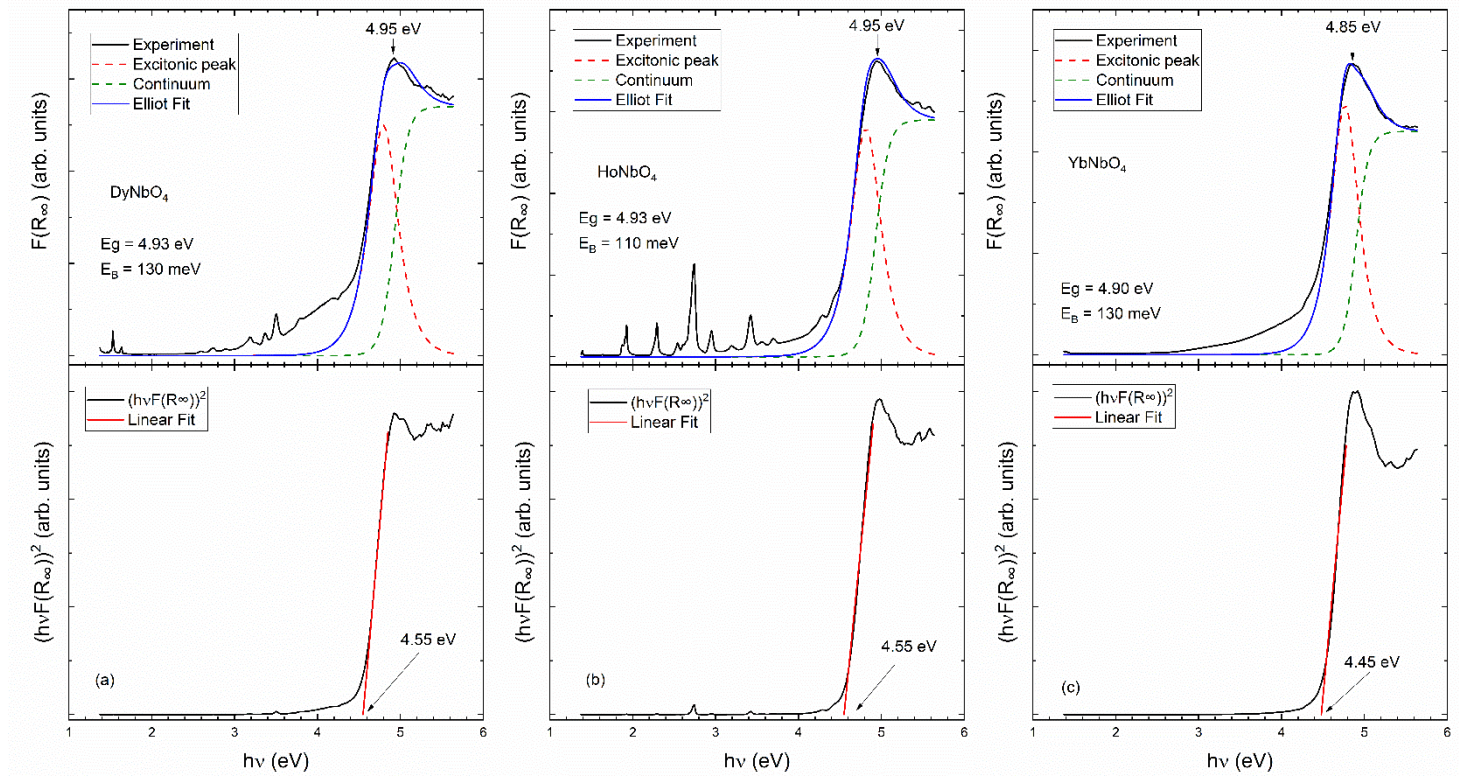


Figure 3: (a) In the top we plot the $F(R_\infty)$ spectrum of DyNbO₄ together with the fit used to determine the band-gap energy. The black line is the experiment, the blue line is the fit, the green dashed line is the continuum contribution, and the red dashed line is the excitonic contribution. In the bottom we show the Tauc plot traditionally used to determine E_{gap} . (b) Same but for HoNbO₄. (c) Same but for YbNbO₄.

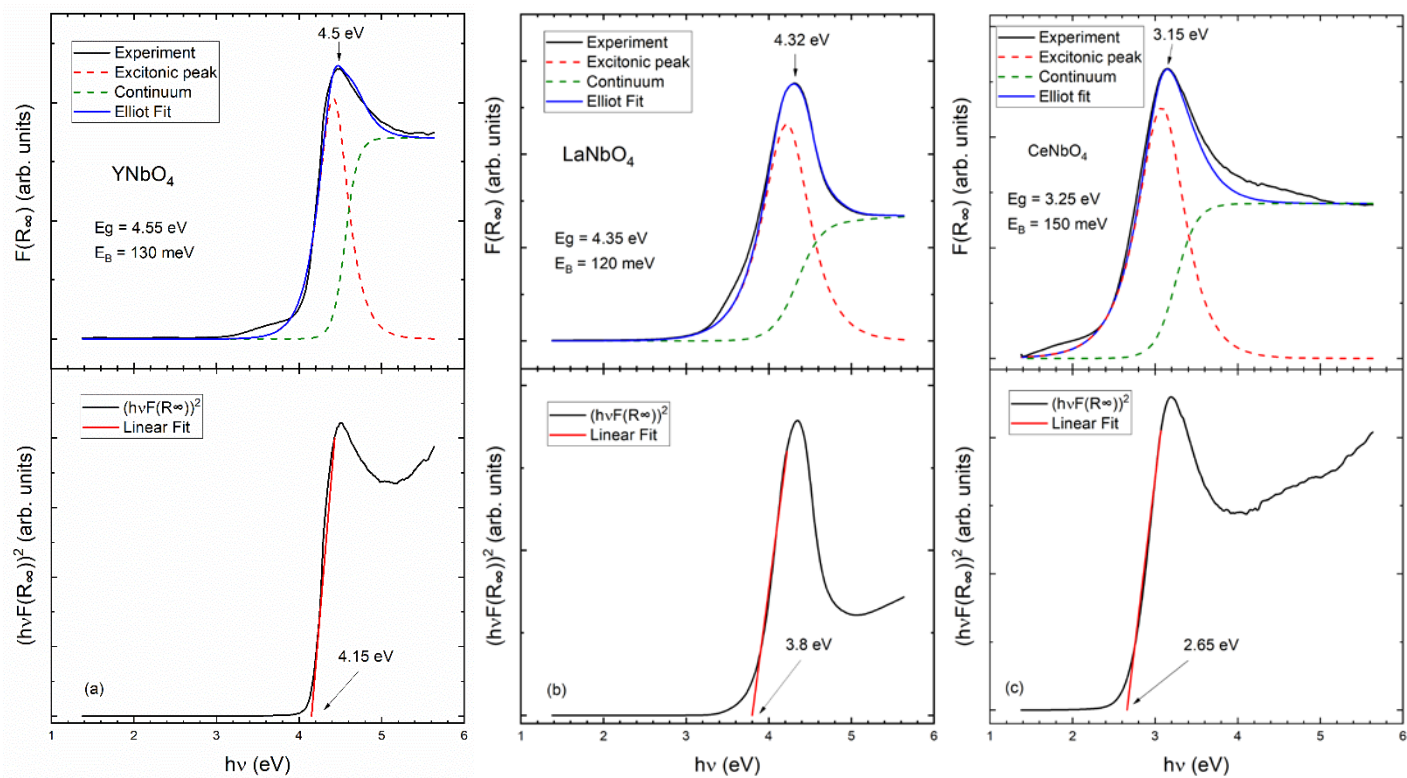


Figure 4: (a) In the top we plot the $F(R_\infty)$ spectrum of YNbO_4 together with the fit used to determine the band-gap energy. The black line is the experiment, the blue line is the fit, the green dashed line is the continuum contribution, and the red dashed line is the excitonic contribution. In the bottom we show the Tauc plot traditionally used to determine E_{gap} . (b) Same but for LaNbO_4 . (c) Same but for CeNbO_4 .

Table 1: Band-gap energy of orthoniobates given in eV. Results obtained using the Elliot model and the Tauc plot are compared with the literature.

Compound	Elliot Fit	Tauc Plot	Literature	Reference
InNbO ₄	4.7	4.35	4.7	[22]
ScNbO ₄	4.8	4.38	4.8	[23]
YNbO ₄	4.55	4.15	3.7 – 4.96	[2, 4, 5, 14]
LaNbO ₄	4.35	3.80	4.0	[13]
CeNbO ₄	3.25	2.65		
PrNbO ₄			4.8	[15]
NdNbO ₄				
SmNbO ₄	4.95	4.45	4.7 - 5.0	[33]
EuNbO ₄	4.73	4.30	3.45	[12]
GdNbO ₄	4.93	4.50	3.48 – 4.89	[4, 12]
TbNbO ₄			2.9	[5]
DyNbO ₄	4.93	4.55		
HoNbO ₄	4.93	4.55		
ErNbO ₄			3.5	[16]
TmNbO ₄				
YbNbO ₄	4.90	4.45	3.46	[16]
LuNbO ₄			4.2 – 5.04	[2, 4]